

JET-P(88)48

E. Lazzaro, K. Avinash, N. Gottardi, P. Smeulders  
and JET Team

# Relaxation Model of H-modes in JET

# Relaxation Model of H-modes in JET

E. Lazzaro, K. Avinash, N. Gottardi, P. Smeulders  
and JET Team\*

*JET-Joint Undertaking, Culham Science Centre, OX14 3DB, Abingdon, UK*

\* See annex of P. Lallia et al, "Plasma Heating in JET",  
(13th EPS Conference on Controlled Fusion and Plasma Physics, Schliersee, Germany (1986)).

Preprint of Paper to be submitted for publication in  
Nuclear Fusion

“This document contains JET information in a form not yet suitable for publication. The report has been prepared primarily for discussion and information within the JET Project and the Associations. It must not be quoted in publications or in Abstract Journals. External distribution requires approval from the Publications Officer, JET Joint Undertaking, Abingdon, Oxon, OX14 3EA, UK”.

“Enquiries about Copyright and reproduction should be addressed to the Publications Officer, EFDA, Culham Science Centre, Abingdon, Oxon, OX14 3DB, UK.”

The contents of this preprint and all other JET EFDA Preprints and Conference Papers are available to view online free at [www.iop.org/Jet](http://www.iop.org/Jet). This site has full search facilities and e-mail alert options. The diagrams contained within the PDFs on this site are hyperlinked from the year 1996 onwards.



## RELAXATION MODEL OF H-MODES IN JET

E. Lazzaro, K. Avinash, N. Gottardi and P. Smeulders

### ABSTRACT

Several phenomenological aspects of H-modes are described using a single variational principle. The observed dependence of global confinement time on current and the characteristics of local heat diffusivity for a relaxed energy state are discussed.

### I. INTRODUCTION

The improvement of the mode of operation and of the design of the JET poloidal field system has allowed (LAZZARO et al., 1985, 1986; TANGA et al., 1987, 1988) the production of single null magnetic separatrix configurations at currents up to 5 MA, with high energy confinement under intense neutral beam heating.

The high confinement regime, first discovered in ASDEX (WAGNER et al.) and called H-mode, appears as a transition from low (L) confinement regime. In JET it is triggered when the additional (NBI) power exceeds about 2.5 times the ohmic power and the boundary conditions on the heat flux, controlled by the magnetic separatrix, allow the formation of edge temperature and pressure pedestals (WAGNER et al., 1985).

The characteristic signatures of H-modes, as observed in several experiments (WAGNER et al.; KEILHACKER et al., 1984, 1987), are: a drop in  $D_{\alpha}$  emissions, a sharp increase in density, an increase in energy content, rather flat temperature profiles with sharp gradients at the boundary and a quiescent MHD activity.

A significant difference between JET-H modes and those of ASDEX is the persistence in JET of sawtooth conditions with  $q(0) < 1$  across the L-H transition.

In ASDEX the disappearance of sawteeth was related to a flattening of the current, indicated by a reduction of the internal inductance.

An analysis of the X-ray emission signals (SMEULDERS et al., 1987), of the interferometric and LIDAR measurements (GOWERS et al., 1988) of the electron temperature, and pressure profiles consistent with the magnetic equilibrium, shows that JET H-modes are often characterised by a long quasi steady state condition with unconventional density and pressure profiles which generally are very flat or hollow within the  $q = 1$  surface.

The pressure and current profiles obtained in this class of H mode allow sawtoothing, with  $q(0) < 1$ , while keeping stability against localised instabilities in the low shear plasma core, according to the Mercier criterion.

Recently it has been surmised (KADOMTSEV, 1986; BISKAMP, 1986; HSU et al., 1987) that the tokamak plasma state could be regarded as one of minimum energy and hence should be obtained via an appropriate variational principle. This approach is along the lines of relaxation theory for RFP (reverse field pinch) where plasma seeks minimum energy state keeping total helicity constant (TAYLOR, 1974). This theory cannot be applied to a non-disruptive tokamak discharge because a minimum energy state under the constraint on total helicity leads to complete magnetic reconnection which occurs only at the time of major disruption. In the quoted papers the authors have minimised the plasma total energy keeping the total plasma current fixed. This yields "relaxed" equilibrium where  $p, J \propto 1/q^2$  (where  $p$ ,  $J$  and  $q$  are the local pressure, current density and safety factor respectively). This equilibrium has finite pressure and current density at the nominal plasma boundary and hence cannot correspond to the L-mode. It seems more like an H-mode

equilibrium which generally features pressure and current density pedestals at the nominal plasma boundary. . Indeed, in JET H-mode there is a definite evidence that pressure and current density profiles are related in this way in the confinement zone. However, in the plasma core this picture is still not consistent with the experimental observation on JET. As stated earlier the JET H-mode is always sawtoothing, hence the core corresponds to an equilibrium with degraded confinement which can be obtained by minimising the energy keeping the core helicity fixed.

Hence, in order to account for the sawtooth we present an extended version of this theory where we propose to do the following:

- (a) Within the mixing radius we minimize the free energy, keeping the helicity within the mixing radius fixed (L-mode).
- (b) Within the confinement zone we minimize the energy, keeping the total current within this region fixed.
- (c) The two equilibria are matched at the mixing radius.

The total current in the outer region is constant over the resistive skin time which is much longer than the sawtooth crash time for which the core helicity is constant. However we are looking for an equilibrium over resistive skin time over which the sawtooth mixing produces an average equilibrium with flat profiles so that the two constraints can be considered together. Local helicity in the confinement region is of course fixed, but cannot be used as a constraint because as such would not allow reaching a (unique) relaxed state.

In this context we further show that in the  $\beta_p \sim 1$  limit, bifurcation of the equilibrium occurs, describing JET and ASDEX types of H mode. Finally some properties and implication of these profiles for the local and global heat transport are discussed. It should be noted that in order to obtain

L-mode equilibrium with zero current at the plasma boundary, Kadomtsev has also considered minimization of plasma energy, keeping the two constraints i.e. the total plasma current and the total helicity constant. However, since total helicity permits mixing within the whole plasma volume which is certainly not the case in a non-disruptive discharge, it is not quite clear how it can be regarded as a constraint over the plasma volume.

The plan of the paper is as follows. In the next section we present a brief account of minimization of potential energy with two constraints. In section III bifurcation of solution is discussed. In section IV and V the implications for global and local transport are presented. Section VI and VII present the comparison with experiments and the discussion.

## II. MINIMISATION OF THE PLASMA FREE ENERGY WITH DIFFERENT CONSTRAINTS IN TWO RADIAL ZONES

In our model the plasma is divided in two regions, the mixing region (core) within the  $q = 1$  surface, and the confinement region. In the two plasma regions equilibrium is demanded, and we take the realistic approach of imposing in the two separate regions the "diagnosed" integrals of motion, namely the helicity  $K = \int \underline{A} \cdot \underline{B} dV$  in the core and the current  $I = \int J ds$  in the confinement region. The plasma total energy

$$W = \int dV \left\{ [F^2 + (\nabla\psi)^2] / 2\mu_0 R^2 + \frac{P}{\gamma-1} \right\} \quad (1)$$

is then minimised under these constraints.

Here  $\frac{F}{R} = B_T$  is the toroidal field,  $\psi(R,Z)$  is the poloidal field stream function,  $P$  is the pressure and  $\gamma$  is the ratio of specific heats. The minimisation of (1) in the confinement region outside the mixing surface  $\psi_s$  ( $q = 1$ ) is performed with constant current constraint  $I$



$$I = \int (FF'/R + RP') \frac{dV}{2\pi R} \quad (2)$$

and the Grad Shafranov equilibrium equation

$$R^2 \nabla \cdot (R^{-2} \nabla \psi) = - \mu_0 (FF' + R^2 P') \quad (3)$$

Following Hsu et al (HSU, 1987) we consider variations of  $\psi$  vanishing at  $r = a$  and assuming that the fluid moves in such a way that the functional dependence of  $F$  and  $P$  on  $\psi$  is not changed. Using a Lagrange multiplier  $\lambda$ , the variational principle can be expressed as:

$$\delta(W + \lambda I) = 0 \quad (4)$$

Substituting Eqs.(1), (2) and (3) in Eq.(4) gives pressure and current density profiles in toroidal geometry as:

$$\frac{dp}{d\psi} = C_p e^{\frac{5}{4\lambda} \psi} \quad (5)$$

$$J_\phi = RC_p e^{\frac{5}{4\lambda} \psi} + \frac{C_F}{R} e^{\psi/\lambda} \quad (6)$$

We consider here a high  $\beta_p = \frac{\langle p \rangle}{B_\theta^2 / 2\mu_0}$  H-mode situation, in which it is legitimate to consider the paramagnetic term  $C_F \cong 0$  and furthermore we consider Eqs.(3,5,6) in the large aspect ratio approximation. Using pseudo cylindrical coordinates  $(r, \theta, z)$  we obtain an equilibrium equation of the Liouville type:

$$\frac{1}{r} \frac{d}{dr} r \frac{d\psi}{dr} + \frac{1}{r^2} \frac{\partial^2 \psi}{\partial \theta^2} = - \mu_0 C_p R^2 e^{\psi/\lambda} \quad (7)$$

where  $\lambda$  has been redefined as  $\frac{5}{4} \lambda \rightarrow \lambda$ .

In general this equation admits multiple solutions (MONTGOMERY et al., 1979; TRACY, 1987) for given boundary conditions.

For azimuthally symmetric case Eq.(7) can be expressed in dimensionless form as

$$\frac{d}{dx} xy' = - \Lambda x e^y \quad (8)$$

with  $x = r/a$ ,  $y = \psi/\lambda$ ,  $\Lambda = \frac{C R^2 a^2 \mu_0}{P \lambda}$ . The solution which matches the solution in the mixing region (at  $r = r_s$ ,  $\psi = \psi_s$ ) can be expressed as

$$y = y_s + \ln \left[ \frac{(1 + \alpha x_s^2)^2}{(1 + \alpha x^2)^2} \right] \quad (9)$$

where  $y_s = \psi_s/\lambda$ ,  $x_s = r_s/a$  and  $\alpha$  is a constant to be evaluated as follows:

From Eqs.(8) and (9)

$$\frac{1}{x} \frac{d}{dx} (xy') \Big|_{x=x_s} = - \frac{8\alpha}{(1 + \alpha x_s^2)^2} = - \Lambda e^{y_s} \quad (10)$$

Imposing the boundary condition  $y = 0$  at  $x = 1$

$$(1 + \alpha x_s^2)^2 e^{y_s} = (1 + \alpha)^2 \quad (11)$$

and

$$\alpha = \frac{\Lambda}{8} (1 + \alpha)^2 \quad (12)$$

which possess real solutions of  $\alpha$  for  $\Lambda < 2$ .

Now Eqs.(11) and (9) imply

$$y = \lambda n \frac{(1 + \alpha)^2}{(1 + \alpha x^2)^2} \quad (13)$$

Hence the current density  $J_z$  in the range  $r_s < r < a$  is given by:

$$J_z = RC_p \frac{(1 + \alpha)^2}{(1 + \alpha x^2)^2} \quad (14)$$

and the associated poloidal field  $B_\theta$  turns out to be

$$B_\theta = -\frac{a}{x} \mu_o RC_p \frac{(1 + \alpha)^2}{2\alpha} \frac{1}{(1 + \alpha x^2)} + \frac{C}{ax} \quad (15)$$

where  $C$  is a constant which is to be determined by matching  $B_\theta$  at  $x_s$  with the  $B_\theta$  in the mixing region. It should be noted that this core equilibrium is only an average equilibrium over many sawtooth crashes. Within this region ( $0 < r < r_s$ ) the energy is minimised keeping constant the helicity

$$K = \int_{V_s} \underline{A} \cdot \underline{B} dV \quad (16)$$

within the volume of the mixing region. In Eq.(16)  $\underline{A}$  is the vector potential and  $\underline{B}$  is the magnetic field. The variational principle in the mixing region is expressed by:

$$\delta \int \left[ \frac{B^2}{2\mu_o} + \frac{P}{\gamma-1} + \nu \underline{A} \cdot \underline{B} \right] dV = 0 \quad (17)$$

where  $\nu$  a Lagrange multiplier and integration is over the volume of the mixing. Together with Ampere's law the solution of Eq.(17) gives:

$$J_z = \nu B_z$$

$$J_{\theta} = vB_{\theta}$$

$$0 < r < r_s$$

$$p = p_0$$

$$B_z = B_T J_0(vr)$$

$$B_{\theta} = B_T J_1(vr) \quad (18)$$

with  $J_0, J_1$  ordinary Bessel functions. In the limit  $vr \ll 1$  we obtain

$$B_z = B_T$$

$$J_z = vB_z = J_{z0} = \text{const}$$

$$B_{\theta} = B_T v \frac{r}{2} = J_{z0} \frac{r}{2} \quad \text{for } r < r_s$$

$$q = q_0 = 2/\mu_0 Rv \quad (19)$$

and with the gauge choice  $A_z = \psi = \psi_s$  at  $r = r_s$ . Matching  $B_{\theta}$  in the two regions at  $x = x_s$  specifies the constant in Eq.(15) giving  $B_{\theta}$  and  $q$  in the confinement zone  $x_s < x < 1$  as:

$$B_{\theta} = \frac{a}{2x} \mu_0 J_{z0} \left[ \frac{x^2 - x_s^2}{(1 + \alpha x^2)} + x_s^2 \right] \quad (20)$$

$$J_{z0} = \frac{C}{P} R(1 + \alpha)^2 / (1 + \alpha x_s^2)^2$$

$$q = \frac{\alpha x B_T}{R B_{\theta}} = \frac{q_0 (1 + \alpha x^2)}{(1 + \alpha x_s^2)} \quad (21)$$

$$\text{for } r_s < r < a \text{ with } q_o = \frac{2B_T}{\mu_o R J_{zo}} \quad (22)$$

It should be noted that the definition of  $q_a$  is in terms of  $B_\theta(a)$  and not of the total current  $I_p$ .

From this basic expression it is easy to calculate the other relevant profiles and analyse their properties. Eqs.(14), (19) and (21) imply the general result formally identical to the current density profile obtained in ref. (BISKAMP, KADOMTSEV, HSU et al.)

$$J = J_{zo} \left( \frac{q_o}{q} \right)^2 \quad (23)$$

The pressure profile in  $r_s < r < a$  is obtained from Eqs.(5) and (13)

$$P(\psi) = P(\psi_s) + \frac{\lambda C_p (1 + \alpha)^2}{(1 + \alpha x_s^2)^2} \left[ \frac{(1 + \alpha x_s^2)^2}{(1 + \alpha x^2)^2} - 1 \right] \quad (24)$$

Matching the pressure of the mixing and the confinement regions at  $r = r_s$  i.e.  $p(\psi_s) = p_o$  and considering that H-modes feature pressure pedestals at the boundary  $p(1) \neq 0$  we get

$$P = p_o \left( \frac{q_o}{q} \right)^2 \quad (25)$$

which has a remarkable property of proportionality with the current profile given by Eq.(23). It should be carefully noted that mutual proportionality of current density and pressure profiles is only possible if there is a pressure pedestal at the plasma boundary. For L mode  $p(1) = 0$  in which case

the pressure cannot be expressed as in Eq.(25) and the proportionality between  $p$  and  $J$  no longer holds.

The optimal current profile (23) describes in general a state with a finite current pedestal at the nominal boundary  $r = a$ . There are two interesting limiting cases (HSU, et al., 1987) to discuss:

$$\lim_{\alpha \rightarrow -1} J_z(x=1) = \infty$$

which is a skin current distribution, with no plasma energy contained in the confinement zone, and:

$$\lim_{\alpha \rightarrow \infty} J_z(x) = \frac{I_p}{\pi a^2} \frac{x_s^2}{(2 - x_s^2)} \frac{1}{x^4}.$$

For  $x_s = 0$  this represents a filament of current at  $x = 0$ . If  $x_s \neq 0$  then this shows that all the current is within the mixing radius and decreases very rapidly away from it.

The pedestal value of the pressure at constant  $B_z$  increases as the square of the total current

$$P_a = p_0 \left( \frac{q_0}{q_a} \right)^2 \propto I_p^2 p_0 \quad (26)$$

suggesting that ohmic H-modes are possible at high current (and in sawtooth conditions).

### III. BIFURCATION OF H-MODE EQUILIBRIUM

The complete specification of the relaxed model follows from a number of

relations among the six undetermined constants  $C_p$ ,  $\Lambda$ ,  $\alpha$ ,  $\lambda$ ,  $\langle p \rangle$ ,  $x_s$ , and quantities which can be considered as assigned, i.e.  $\beta_o = \frac{2\mu_o p_o}{B_o^2(a)}$ ,  $q_o (= 1)$  and  $q(a)$ . These can be obtained, with some algebra, from Eqs.(14) to (24). Thus we have

$$\frac{\lambda\Lambda}{C_p} = \mu_o R^2 a^2 \quad (27)$$

$$C_p \langle P \rangle = \frac{I P_o}{\pi a^2 R q_a^2} \quad (28)$$

$$\lambda C_p = \frac{q_a^2}{P_o} \quad (29)$$

$$x_s = \left[ \frac{\langle P \rangle}{P_o} - \frac{1}{q_a} \right]^{\frac{1}{2}} \quad (30)$$

$$\alpha = \frac{q_a - 1}{1 - q_a x_s^2} \quad (31)$$

The closing equation is provided by Eq.(12)

$$\alpha = \frac{\Lambda}{8} (1 + \alpha)^2 \quad (32)$$

Thus we have a set of six relations for six unknowns.

By eliminating  $C_p$  and  $\lambda$  between Eqs.(27)-(29) we obtain

$$\Lambda = \frac{8}{\beta_o q_a^2} \frac{P_o^2}{\langle P \rangle^2} \quad (33)$$

It has already been stated that Eq.(7) has multiple solutions. As a matter of fact Eq.(33) with expressions (27-31) leads to a bifurcation equation for the peakedness parameter  $\frac{\langle P \rangle}{P_0}$  which is

$$\left(\frac{\langle P \rangle}{P_0}\right)^2 - \frac{\langle P \rangle}{P_0} + \frac{1}{\beta_0} = 0 \quad (34)$$

If  $\beta_0 > 4$  then Eq.(34) has two real solutions for  $\frac{\langle P \rangle}{P_0}$ .

The solution with smaller  $\frac{\langle P \rangle}{P_0}$  can be interpreted from Eq.(30) as an "ASDEX" type H-mode, with vanishing or imaginary  $x_s$  and no sawteeth. The JET sawtooth type of H-mode can be identified with the larger  $\frac{\langle P \rangle}{P_0}$  (and finite  $x_s$ ) solution.

We remark that the bifurcation disappears if the pressure pedestal vanishes, and that JET and ASDEX different sawtooth conditions might also be related to the different geometric shear due to the non circular cross section, which here is neglected.

#### IV. CONSEQUENCES OF THE MODEL FOR GLOBAL TRANSPORT

The achievement of a relaxed state where the energy pressure profile is fixed as a function of  $q$ , implies that the plasma thermal energy content

$$W = \int dV \frac{3}{2} n (T_e + T_i) = 12\pi^2 R \int_0^a dr r P(r)$$

from Eq.(25) can be written as

$$W = 6\pi^2 a^2 R P_0 \frac{q_0}{q_a}$$



and the global energy replacement time is

$$\tau_E = \frac{W}{P_{ow}} = 6\pi\mu_0 R^2 \frac{q_0 I_p}{B_z} \frac{P_0}{P_{ow}} \quad (35)$$

The dependence on the input power  $P_{ow}$  can then only be through  $P_0$ , for a given total current  $I_p$  and toroidal field  $B_z$ .

Experimentally it is observed (KEILHACKER, 1987; ODAJIMA, 1988) that the confinement time in H-modes (and high density regimes) is proportional to the total current while still degrading with increasing input power. Although an absolute scaling of the confinement time at this stage is impossible, this observation can be reconciled with expression (35) if it is assumed that the heating efficiency, which depends on the input power deposition profiles is such that  $P_0 = C_0 P_{ow}^\sigma$  with  $\sigma \leq 1$ , and  $C_0$  depends only on  $B_z$ . The assumptions that reconcile Eq.(35) with the experimental evidence, also imply that the edge value of the pressure scales as:

$$P_a \propto P_{ow}^\sigma I_p^2 / B_z$$

Therefore for H-modes with the same current to obtain the same pedestal value  $p_a$  the required power scales as:

$$P_{ow} \propto B_z^{1/\sigma}$$

With a typical  $\sigma = 0.4$  this scaling is in agreement with the experimental results (KEILHACKER et al., 1987). By considering Ohm's law and the profile (23) for the current density the expected dependence of the electron temperature profile is:

$$T_e = T_o (q_o/q)^{4/3}$$

Figs.8 and 9 show two examples of experimental (LIDAR) temperature data plotted versus  $q$  and the corresponding best fitting curve. It appears that the theoretical model fits well within 10% in the H phase. The bad fitting shown in Fig.10 is for an L state.

#### V. LOCAL TRANSPORT WITH CANONICAL PROFILES

We consider here in an elementary way the implications for the local transport of a relaxed equilibrium described by the profiles (23,25).

Considering, as appropriate a steady state energy balance equation (with  $T_e \sim T_i$ ) we can write the heat flux across a generic surface of radius  $r$  as:

$$-rn\chi \frac{dT}{dr} = -\delta rn\chi T_o n_o \left(\frac{q_o}{q}\right)^2 \frac{q'}{q} = \int r Q(r) dr \quad (36)$$

where  $Q(r)$  is the net power input per unit volume. As a consequence of the canonical current and pressure profiles and of relations between current and temperature (of ohmic type) or between pressure and density (state equations) it is expected that  $T$  will depend on  $q^{-\delta}$  and  $n$  on  $q^{\delta-2}$  with  $\delta$  a real exponent.

By splitting the net power input per unit volume  $Q$  as

$$Q = \eta J^2 + Q_{aux},$$

where  $Q_{aux}$  is the net auxiliary heating input, one gets from Eq.(36) a tautological expression for the heat diffusivity profile

$$\chi = \frac{1}{\delta n T} \left(\frac{q}{r q'}\right) \int \eta J^2 r' dr' \left[1 + \frac{\int Q_{aux}(r') r' dr'}{\int \eta J^2 r' dr'}\right] \quad (37)$$

which is similar to that used by Coppi in the presentation of the profile consistency principle (COPPI, 1980). In the case of Ohm's law  $\delta = 4/3$ .

Unfortunately no absolute scaling or dependence of  $\chi$  on density temperature and radius can be read from expressions such as Eq.(37).

However, the inverse dependence of  $\chi$  on the current density shear is in agreement with the picture of  $\chi \rightarrow \infty$  in the mixing region, which after a sawtooth crash is ideally shearless. In the confinement region ( $r_s < r < a$ )  $\chi$  is a monotonic increasing function of  $q$ .

For strong auxiliary heating the space dependence of  $\chi$  and the resulting incremental confinement time depend on the auxiliary power deposition profiles, and the absorption mechanism.

The discussion of these effects will be presented in a subsequent work carried out with transport codes using expression (37).

## VI. EXPERIMENTAL EVIDENCE

Hollow X-ray emission profiles with maximum around the sawtooth inversion radius are generally observed in JET X-point discharges. Fig.1 shows the time evolution of the X-ray emission in the torus midplane as a function of radius. The hollowness varies gradually in time, with periodic deepening after each sawtooth collapse.

After transition to the H mode at 12.2 sec. the profiles remain hollow or flat over the whole H mode period.

Correlated with the hollow X-ray profiles, are hollow plasma density profiles, as shown in Fig.2. While X-ray and density profiles are flat or hollow, the ECE and LIDAR measurements of electron temperature give flat or peaked, but broad profiles.

The LIDAR measurements of electron pressure is generally flat or hollow during the H-mode, as shown for instance in Fig.3.

A self consistent calculation of plasma equilibrium using the experimental pressure profile and best fitting the magnetic and diamagnetic signals gives a safety factor profile with a wide, nearly shearless region with  $q < 1$ , in agreement with the observed sawtooth condition, as shown in Fig.4. Details of the experimental measurement are given in (SMEULDERS et al., 1987). Similar results have been observed in DIII-D (STAMBAUGH et al., 1988).

The interesting aspect of these results in comparison with the theory presented, is shown in Figs.5 and 6. Here the actual current and pressure profiles for the L-H transition in shot 10766 are plotted against the theoretical model of Eqs.(23), (25). It appears that over most of the plasma cross section the experimental H mode pressure and current profiles follow the  $1/q^2$  behaviour. During the L phase the pressure has a visibly different behaviour, while the current  $J$  appears already close to the  $1/q^2$  dependence.

Figure 7 shows the dependence of the experimental global confinement time  $\tau_E$  versus  $1/q_a$ , which follows closely the prediction of Eq.(35).

## VII. SUMMARY AND CONCLUSIONS

In this paper we have shown that it is possible to describe sawteething H-modes as those observed in JET and DIII-D from a single variational principle, which yields unique profiles of current and pressure, proportional to  $1/q^2$  even if a mixing region exists.

Many authors have shown that well defined current and pressure profiles are obtained either from stationary entropy principles (MONTGOMERY 1979; PFIRSCH et al., 1986; MINARDI, 1973; REBHAN, 1986) with certain constraints, or by minimising the plasma free energy under constraints (BISKAMP et al., 1986; KADOMTSEV et al., 1986, 1987; HSU et al., 1987). We have adopted a similar relaxation model by making the free energy stationary with a constraint of constant helicity within the mixing surface and constant

current in the confinement zone. The equilibria in the two regions are matched at the mixing radius. In the high  $\beta_p$  limit the solution bifurcates into two equilibria with different radii of inversion. We identify the equilibrium with larger radius of inversion with that of JET and that with the vanishing inversion radius could be of the type observed in ASDEX, which is sawtooth free.

The mutual proportionality of the current and pressure profiles and the bifurcation of solution is shown to be a strict consequence of the finite pressure pedestal. In the original work of Kadomtsev which considered essentially unbounded plasmas, the current and pressure had the same dependence and proportionality but solutions were not bifurcated. The pressure pedestal value depends directly on the square of the total current  $I_p$ , indicating the possibility of H-type equilibria at higher currents, in agreement with some recent evidence of Ohmic H-modes (DIII-D).

The accessibility of H-mode equilibria, with finite pedestals, from L-mode with vanishing edge pressure and current depends on matching the edge heat and particle flows with flows along the open field lines of a divertor configuration in an edge plasma region presently not considered. The spontaneous transition to a temperature pedestal has been considered by Rebut (REBUT et al., 1988) as a consequence of exchange of roles of ion and electron transport near the separatrix. Other models of transport in the scrape-off region justify the formation of pedestals by variation of the boundary conditions (HINTON, 1986; ITOH, 1988), but a complete description is still an open problem. Interesting implications of the H-modes profiles for local and global transport have been found. In particular, for local transport the general properties of the local heat conductivity appear in accordance with Coppi's original explanation of profile consistency for L-mode discharges, and suggest a similar consistency principle for H-modes. For global transport the observed dependence of  $\tau_E \propto I_p$  implies in our model a dependence of the

central pressure  $p_0$  only on the heating power and the toroidal field  $B_2$ .

Finally it should be noted that the model of Biskamp and Kadomtsev were originally proposed to justify profile consistency in tokamaks. The profiles obtained however cannot correspond to L-modes because of the finite pedestals. Further work by Kadomtsev to describe L-modes from minimisation of energy under total current and helicity constraints in the whole plasma region produces current profiles  $\propto [\frac{A}{q^2} + \frac{B}{q} + C]$  for which there is no convincing experimental evidence.

From recent analysis of experimental observations (NAVE, LAZZARO et al., 1988) it appears more likely that the L-mode be a state of saturated nonlinear tearing modes, which develops flat (force free) regions on the pressure profile, at the location of rational  $q$  surfaces. This theoretical model will be fully discussed elsewhere.

#### ACKNOWLEDGEMENTS

Two of the authors (K. Avinash and E. Lazzaro) are grateful to Dr. M. Keilhacker, Prof. B. Kadomtsev, G.V. Pereverzev, K. Lackner and T. Stringer for useful discussions.

## REFERENCES

- BISKAMP, D. Preprint IPP/6/258 Max-Planck Institute für Plasmaphysik 1986.
- COPPI, B. Comments on Plasma Phys. and Contr. Fus. 5 261 (1980).
- EDENSTRASSER, J.W., HOHENAUER, W.M.M. 15th EPS Conf. Vol.I, 433.
- GOWERS, C., BARTLETT, D., BOILEAU, A. et al., Profile behaviour during L and H phases of JET discharges. Proceed. 15th EPS Conf. on Contr. Fus. and Plasma Heating, Dubrovnik 1988, Vol.I, 239.
- HINTON, F.L. Nucl. Fus. 25 1457 (1985)
- HSU, J.Y., CHU, M.S. Phys. Fluids 30 1221 (1987).
- ITOH, S., ITOH, K. Phys. Rev. Lett. 22 2276 (1988).
- KADOMTSEV, B.B. Phil. Trans. R. Soc. Lond. A 322, 125 (1987).
- KADOMTSEV, B.B. Sov. J. Plasma Phys. 13 (7) 443 (1987).
- KEILHACKER, M. et al. JET Report P(87)36.
- KEILHACKER, M. et al. Plasma Phys. and Contr. Fus. 49 26 (1984).
- LAZZARO, E. et al. Magnetic Separatrix Formation in JET. 27 APS Meeting, San Diego, 4-8 Nov. 1985, BAPS 8F1, 1585.
- LAZZARO, E. et al. Magnetic Separatrix Operation in JET. 28 APS Meeting, Baltimore, 3-7 Nov. 1986, BAPS 5E11, 1503.
- MINARDI, E. Workshop on Mirror Based and Field Reversed Approach to Mag. Fus. Int. School of Plasma Physics, Varenna (1983) 41.
- MONTGOMERY, D., TURNER, L., VAHALA, G. J. Plasma Phys. 21 239 (1979).
- NAVE, M.F., LAZZARO, E. et al. 15th EPS Conf. Vol.I, 441.
- ODAJIMA et al. 11th IAEA Conf. on Plasma Phys. and Contr. Fus. A-III-2, Dubrovnik, 1988.
- PFIRSCH, POHL. Plasma Phys. and Contr. Fus. 29 697 (1987).
- REBHAN, E., GRAUER, R. Tokamak profiles through constrained minimization of the entropy production. 14th EPS Conf. on Contr. Fus. and Plasma Phys., Madrid 1987, vol.III, 1072.
- REBUT, P., LALLIA, P., WATKINS, M. 15th EPS Conf., Vol.I, 247.
- SMEULDERS, P. et al. Hollow density profiles during H-modes in JET. 29th APS Meeting, San Diego, 1987, JET-IR(88).
- STAMBAUGH, R., ALLEN, S., BRAMSON, G. et al., Invited paper, 15th EPS Conf. on Contr. Fus., Dubrovnik, 1988.
- TANGA et al. Nucl. Fus. 27 (1987) 1877.
- TANGA et al. Proceed. 15th EPS Conf. on Contr. Fus. Vol.I, 235, Dubrovnik 1988, Vol I, 235.
- TAYLOR, J.B. Phys. Rev. Lett. 33 1139 (1974).
- TRACY, E.R., CHIN, C.H., CHEN, H.H. Physica 23 D91 (1986).
- WAGNER et al. Nucl. Fus. 25 1490 (1985).





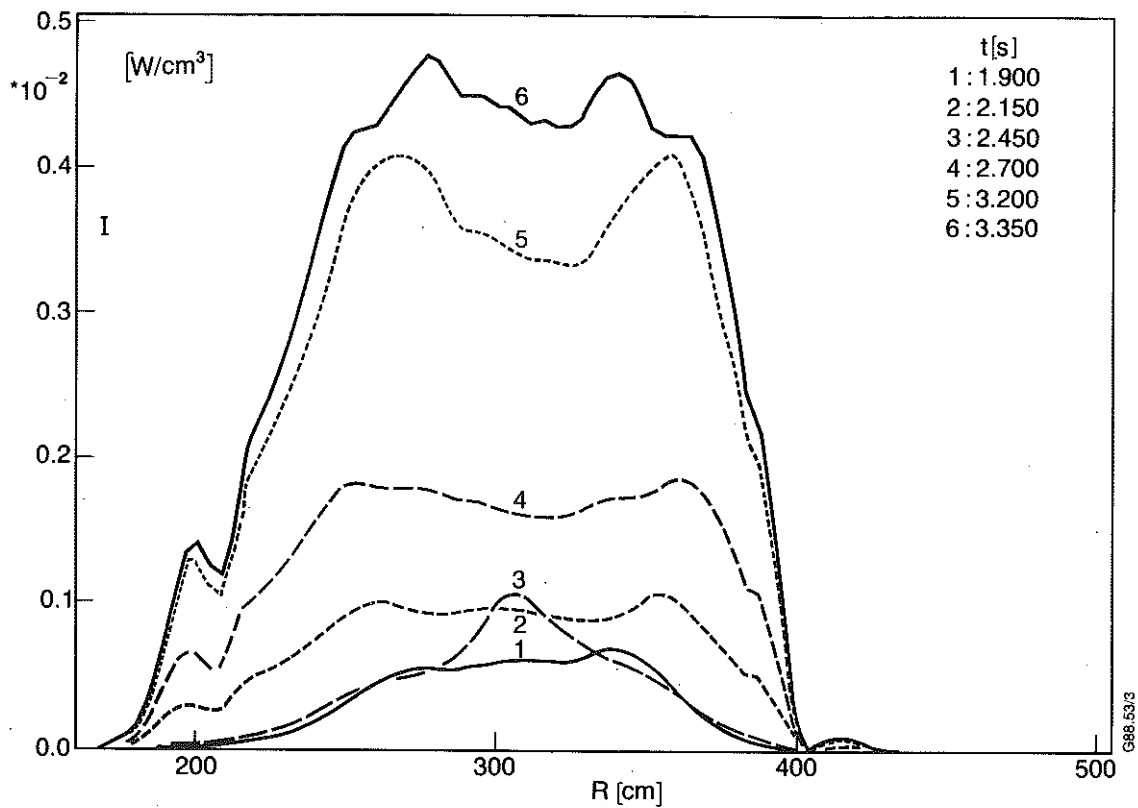


Fig. 1 X-ray emission  $I(R, t)$  in torus midplane from  $t=10.9$  to  $13.4$ s. The L to H-mode transition occurs at  $12.2$ s after the sawtooth crash.  $NI$  steps up its power at  $12$ s and lasts from  $11$  to  $14$ s. Nine sawteeth can be seen over this period.

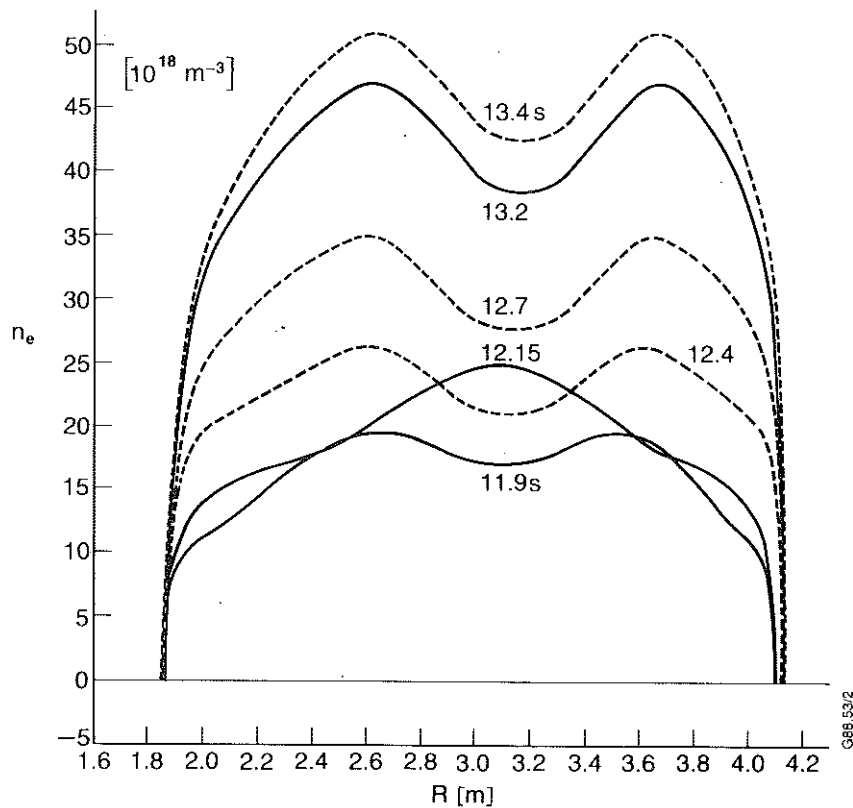


Fig. 2 Abel inverted electron line-densities  $ne(R)$  in torus midplane for various times.

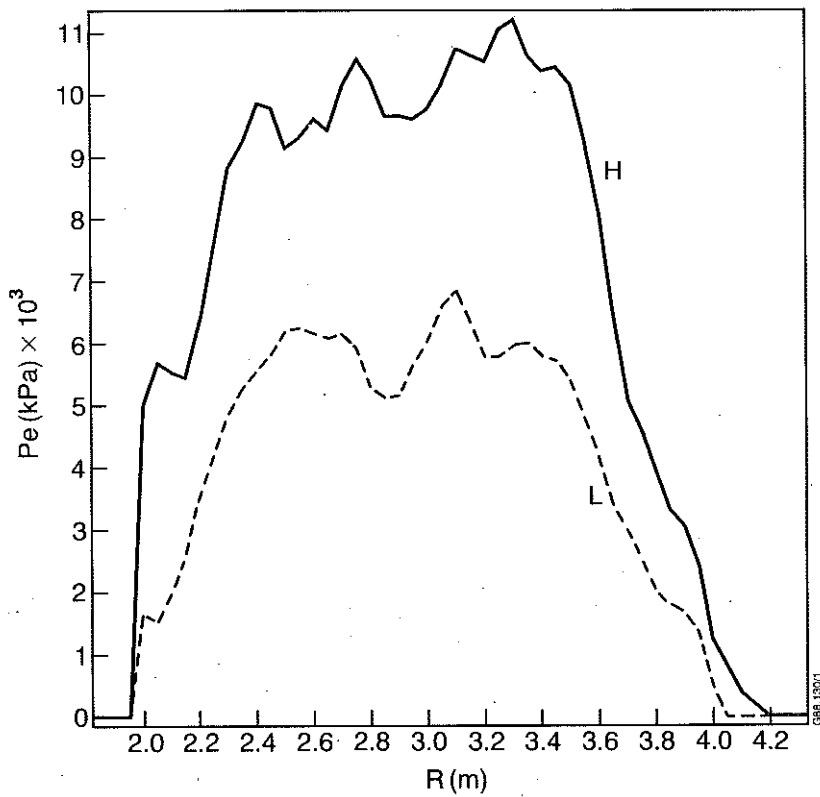


Fig.3 Pressure profiles obtained by the LIDAR diagnostics for L-H transition.

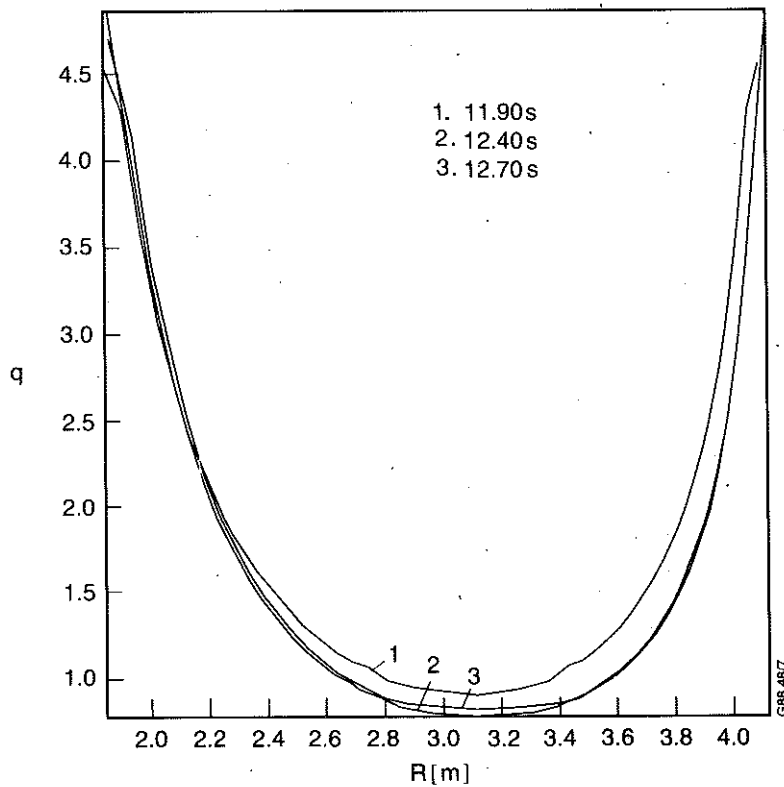


Fig.4 Safety factor profile from equilibrium calculation for three consecutive times in the L-phase at  $t=11.9$ s and in the H-phase at  $t=12.4$  and  $12.7$ s.

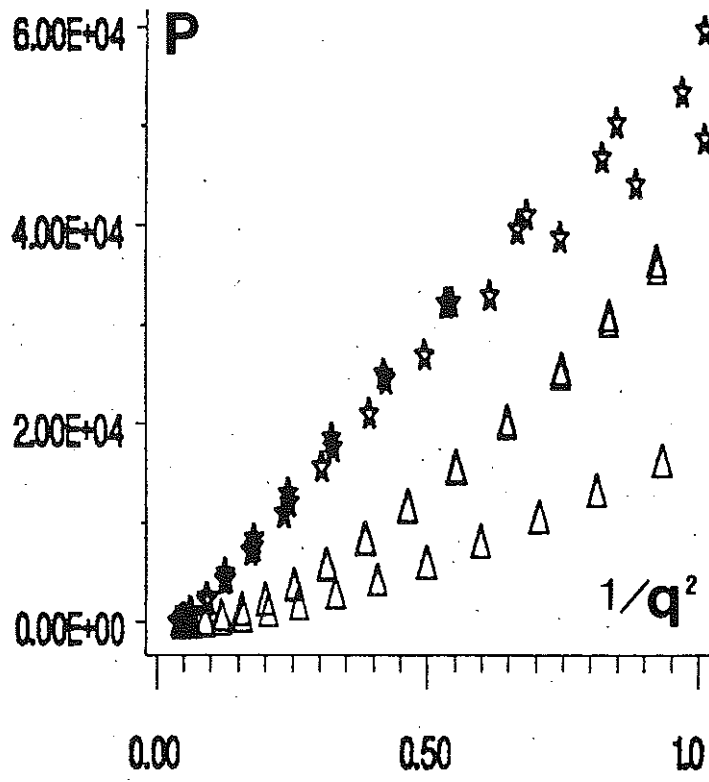


Fig. 5 Equilibrium pressure profile  $p$  of shot 10766 in  $L(\Delta)$  and  $H(*)$  states, plotted versus the theoretical profile  $\propto 1/q^2$  of Eq.(23).

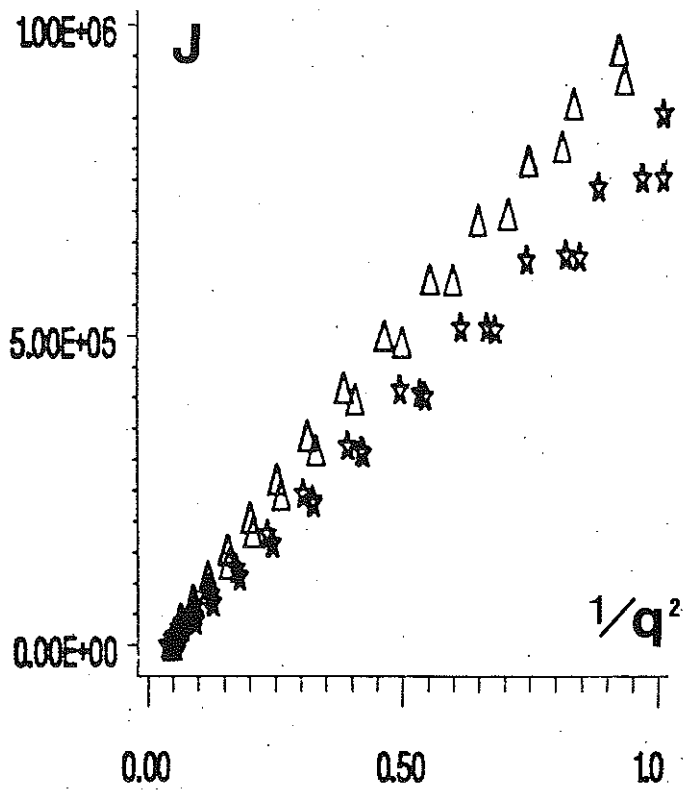


Fig. 6 Equilibrium current density profile  $J$  of shot 10766 in the L and H states plotted versus theoretical model of Eq. (23).

H-Mode years 86-87-88,  $dW/P_{tot} < .2$   
 NBI Octant 4, or 4+8, 1 point per Shot & Power

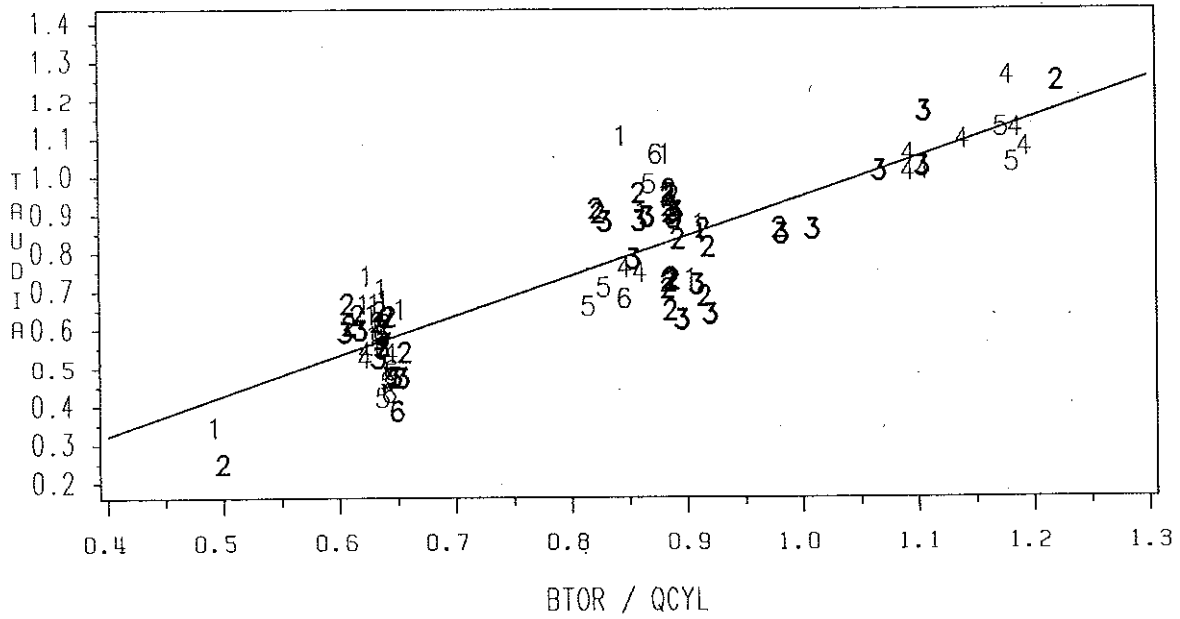


Fig. 7 Dependence of the global confinement time  $\tau_E$  on  $I_p$  in H-mode discharges, for several neutral beam (NBI) power: the \* label  $3 \langle P_{OW} \rangle 5 \text{ MW}$ ; + label  $5 \langle P_{OW} \rangle 6$ ;  $\Delta \langle P_{OW} \rangle 7$ ;  $\square \langle P_{OW} \rangle 8$ ;  $\circ \langle P_{OW} \rangle 9$ ;  $\times \langle P_{OW} \rangle 4$ . Quasi steady state conditions with  $\frac{1}{P_{OW}} \frac{dW}{dt} < 5\%$ .

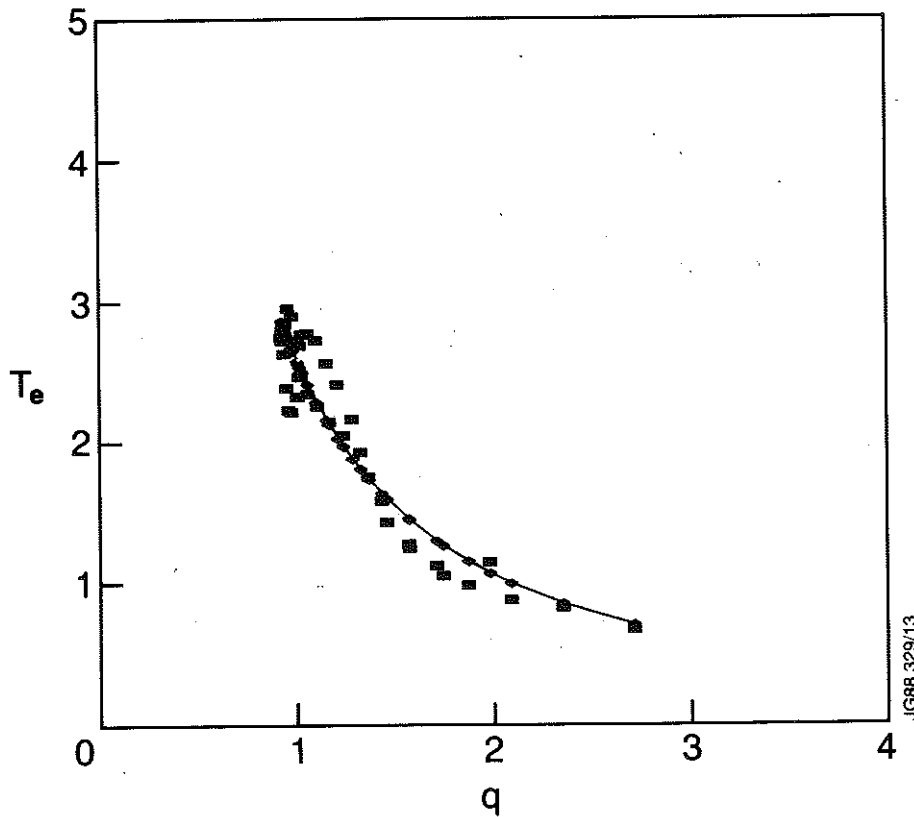


Fig. 8 Best fitting of Experimental Temperature profile of 3 MA H-mode shot 13805, to a power law  $k \cdot q^{-\sigma}$  (expect  $\sigma = 4/3$ , result  $\sigma = 1.3222$ ).

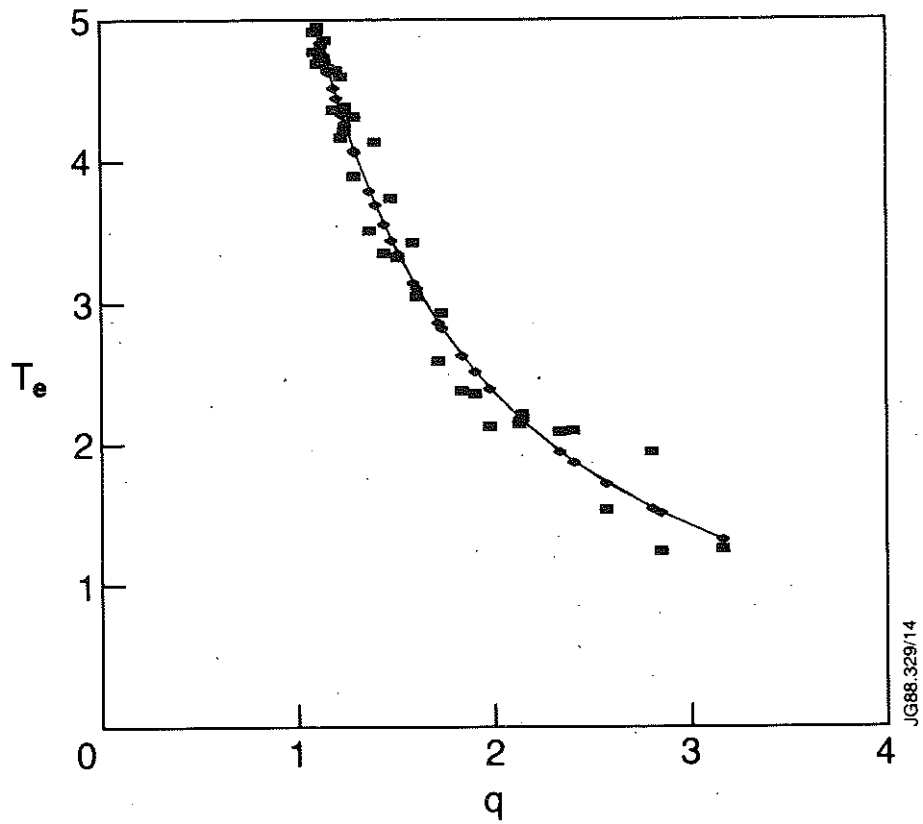


Fig. 9 Same as Fig. 8 for 3MA H-mode shot 15894 (expected  $\sigma=4/3$ , result  $\sigma=1.2934$ ).

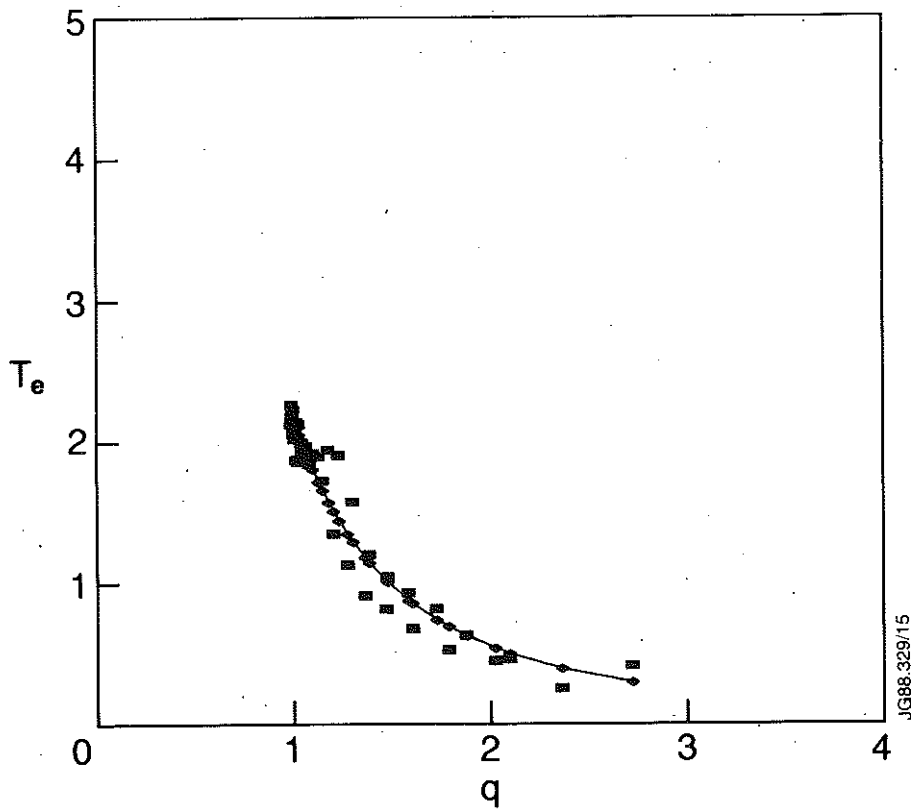


Fig. 10 Same as Fig. 8 for the L-mode phase of shot 13805 ( $\sigma=2.0182$ ).

